[CANCER RESEARCH 64, 3087–3095, May 1, 2004]

Identification and Characterization of a Novel Gene, *C13orf25*, as a Target for 13q31-q32 Amplification in Malignant Lymphoma

Akinobu Ota,[1] Hiroyuki Tagawa,[1] Sivasundaram Karnan,[1] Shinobu Tsuzuki,[1] Abraham Karpas,[2] Shigeki Kira,[3] Yasuko Yoshida,[3] and Masao Seto[1]

[1]Division of Molecular Medicine, Aichi Cancer Center Research Institute, Nagoya, Japan; [2]Department of Hematology, Cambridge University, Medical Research Council Center, Cambridge, United Kingdom; and [3]Geneshot Project, R&D Center, NGK Insulators, Ltd., Nagoya, Japan

ABSTRACT

The amplification at 13q31-q32 has been reported in not only hematopoietic malignancies but also in other solid tumors. We identified previously frequent amplification of chromosomal band 13q31-q32 in 70 cases of diffuse large B-cell lymphoma patients by conventional comparative genomic hybridization analysis. In an attempt to identify a candidate gene within this region, we used array comparative genomic hybridization and fluorescent *in situ* hybridization to map the 13q31-q32 amplicon. We then screened the 65 expressed sequence tags and *Glypican 5* (*GPC5*) by reverse transcription-PCR and Northern blotting. As a result, we identified a novel gene, designated *Chromosome 13 open reading frame 25* (*C13orf25*), which was overexpressed in B-cell lymphoma cell lines and diffuse large B-cell lymphoma patients with 13q31-q32 amplifications. However, *GPC5*, which has been reported to be a target gene for 13q31-q32 amplification, was truncated in one cell line, Rec1, possessing the amplification, and its expression in various cell lines with amplification at 13q31-q32 was not significantly different from that in other cell lines without amplification, suggesting that *GPC5* is not likely to be the candidate gene. Additional analysis identified two major transcripts in the *C13orf25* gene. The two transcripts A and B predicted open reading frames of 32 and 70-amino acid polypeptides, respectively. The former has been reported as *bA121J7.2*, which is conserved among species. Transcript-B also contained seven mature microRNAs in its untranslated region. These results suggest that the *C13orf25* gene is the most likely candidate gene for the 13q31-q32 amplicon found in hematopoietic malignancies.

INTRODUCTION

Chromosomal amplification is a common mechanism by which genes achieve overexpression in tumors. Identification and characterization of oncogenes present in amplified regions can thus provide important insights into the pathogenesis of cancer (1). Activated oncogenes, such as *MYCN* in neuroblastomas or *HER2* in breast cancer, also have prognostic relevance (2–4).

The high-level amplification seen at 13q21-qter has been observed in hematological and other solid neoplasms. Amplification at 13q21-qter has been reported in diffuse large B-cell lymphoma (DLBCL; Ref. 5), mantle cell lymphoma (6), follicular lymphoma (7), primary cutaneous B-cell lymphoma (8), and nasal-type natural killer/T-cell lymphoma (9). Additional cases of amplification at 13q21-qter have also been reported in solid tumors: glioma (10), non-small cell lung cancer (10), bladder cancer (10), squamous-cell carcinoma of the head and neck (10), peripheral nerve sheath tumor (11), malignant fibrous histiocytoma (12), and alveolar rhabdomyosarcoma (13). We also reported the results of cytogenetic analysis of 70 DLBCL patients (14) using conventional comparative genomic hybridization (CGH), which found amplification of 13q, including the 13q31-q32 region, in 18 of 70 DLBCL cases.

Glypican 5 (*GPC5*) has been reported recently as a possible target gene for amplification at 13q31-q32 in a study using fluorescent *in situ* hybridization (FISH) in lymphoma cell lines (15). However, the mRNA expressions of *GPC5* and expression sequence tags (ESTs) located in the amplification region of 13q31-q32 were not dealt with in their study.

In the study presented here, we identified the common region of amplification at 13q31-q32 in DLBCL patients and lymphoma cell lines by CGH, FISH, and array CGH, which allows for rapid screening and more detailed analysis of genomic imbalance in tumor genomes (16–18). This report describes the fine mapping of the 13q31-q32 amplification and identification of a novel gene, designated *C13orf25* (*Chromosome 13 open reading frame 25*) that showed parallel expression to that of genomic amplification of 13q31-q32 in lymphoma cell lines and DLBCL patients. We also provided evidence that *GPC5* is not a likely target for 13q31-q32 amplification.

MATERIALS AND METHODS

Cell Lines, Tumor Specimens, and CGH Method. The cell lines used were Karpas 1718 (splenic lymphoma with villous lymphocytes; Ref. 18), OCI-Ly4, OCI-Ly7, and OCI-ly8 (DLBCL, kindly provided by Dr. Riccardo Dalla-Favera of Columbia University, New York, NY), Rec1 (mantle cell lymphoma, kindly provided by Dr. Martin J. S. Dyer of Leicester University, Leicester, United Kingdom; Ref. 19), Karpas 422 (B-cell lymphoma cell line; Ref. 20), and ATN-1 (adult T-cell lymphoma cell line, kindly provided by Dr. Tomoki Naoe of Nagoya University School of Medicine, Nagoya, Japan; Ref. 21). SUDHL6 (Southwestern University Diffuse Histiocytic Lymphoma cell line; B-cell lymphoma), SP49 (mantle cell lymphoma cell line), Jurkat (T-cell acute lymphocytic leukemia), and other cell lines were described elsewhere (22). Cell lines with variable copy numbers of the X chromosome were purchased from the National Institute of General Medical Sciences Human Genetics Cell Repository Coriell Institute for Medical Research (Camden, NJ). Patient samples were collected with informed consent, and this experiment was approved by the Institutional Review Board of Aichi Cancer Center. All of the cell lines were maintained in RPMI 1640 supplemented with 10% FCS. Genomic DNA was extracted according to standard procedures using proteinase K digestion and phenol chloroform extraction. Normal DNA for use with conventional CGH and array CGH was prepared by using peripheral-blood lymphocytes from a normal male. "Conventional" CGH was carried out according to the manufacturer's protocol (Vysis, Downers Grove, IL).

Array CGH. The array fabrication and hybridization was performed according to the method described by Hodgson *et al.* (23) and Pinkel *et al.* (17), respectively. The array consisted of 2,088 bacterial artificial chromosome (BAC) and P-1 derived artificial chromosome (PAC) clones, covering the human genome at roughly a 1.5-Mb resolution, from library RP11 and 13 for BAC clones and RP1, 3, 4, and 5 for PAC clones. Information on clone names and their location on chromosomes is available on request. These clones were obtained from the BACPAC Resource Center at the Children's Hospital Oakland Research Institute (Oakland, CA).[4] Each clone was cultured in Terrific Broth medium with the chloramphenicol (25 μg/ml), and BAC and

Received 12/3/03; revised 2/5/04; accepted 2/23/04.

Grant support: Grant-in-Aid for the 2nd-Term Comprehensive 10-year Strategy for Cancer Control from the Ministry of Health, Labor and Welfare, a Grant-in-Aid for Science on Primary Areas (Cancer Research) from the Ministry of Education, Science and Culture.

Note: A. Ota and H. Tagawa contributed equally to this work.

The costs of publication of this article were defrayed in part by the payment of page charges. This article must therefore be hereby marked *advertisement* in accordance with 18 U.S.C. Section 1734 solely to indicate this fact.

Requests for reprints: Masao Seto, Division of Molecular Medicine, Aichi Cancer Center Research Institute, 1-1 Kanokoden, Chikusa-ku, Nagoya 464-8681, Japan. Phone: 81-52-762-6111, extension 7080/7082; Fax: 81-52-764-2982; E-mail: mseto@aichi-ml.jp.

[4] Internet address: http://bacpac.chori.org/.

Downloaded from cancerres.aacrjournals.org on March 4, 2021. © 2004 American Association for Cancer Research.

PAC DNA was extracted with a plasmid Mini-kit (Qiagen, Germantown, MD). The location of each clone was also confirmed by FISH analysis. Roughly 10% of these clones could not be assigned to their expected region and excluded from this study, whereas the confirmed clones were used for array CGH. We used 10 ng of BAC and PAC DNA as the template for degenerate oligonucleotide primed PCR with the primer 5′-CCGACTCGAGNNNNNNAT-GTGG-3′, where n = A, C, G, or T (24). Amplifications were performed on a TaKaRa PCR Thermal Cycler MP (TaKaRa, Tokyo, Japan) using ExTaq polymerase (TaKaRa). Degenerate oligonucleotide primed-PCR products were enriched by ethanol precipitation and dissolved in distilled water, and then equal volume of DNA spotting solution DSP0050 (MATSUNAMI, Osaka, Japan) was added (~1 μg/μl). DNA was robotically spotted (NGK Insulators, Ltd., Nagoya, Japan) in duplicate onto CodeLink activated slides (Amersham Biosciences, Piscataway, NJ). Tested and reference DNA (1 μg each) was digested with *Dpn*II and labeled with the Bio prime DNA labeling system (Invitrogen Life Technologies, Inc., Tokyo, Japan) using cyanine3-dUTP and cyanine5-dUTP (Amersham Pharmacia Biotech, Piscataway, NJ), respectively. Unincorporated fluorescent nucleotides were removed with the aid of Sephadex G-50 spin columns (Amersham Biosciences). Labeled 1 μg of tested and reference DNA samples was mixed with 100 μg of Human Cot-1 DNA (Invitrogen Life Technologies, Inc.) and precipitated, after which the pellet was resuspended in the 45-μl hybridization mixture, which consisted of 50% formamide, 10% dextran sulfate, 2× SSC, 4% SDS, and 10 μg/μl yeast tRNA (Invitrogen Life Technologies, Inc.). The hybridization solution was heated to 73°C for 5 min to denature the DNA and then incubated for 45 min at 37°C to allow blocking of the repetitive sequences. The slides spotted with DNA were denatured in a solution consisting of 70% formamide/2× SSC at 73°C for 4 min, then dehydrated in cold 70%, 85%, and 100% ethanol for 5 min each and air-dried. Hybridization was performed for 48 h in a container placed on a slowly rocking table containing 200 μl of 50% formamide and 2× SSC to control moisture. It was followed by 15 min posthybridization washing in 50% formamide/2× SSC at 50°C, 30 min in 2× SSC/0.1% SDS at 50°C, 15 min in PN buffer consisting of 0.1 M NaH_2PO_4, 0.1 M Na_2HPO_4 at (pH 8.0), and 0.1% NP40 at room temperature, rinsing in 2× SSC at room temperature, and finally dehydration in 70%, 85%, 100% ethanol at room temperature for 2 min each and air-drying. Scanning analysis was basically carried out with the Agilent Micro Array Scanner (Agilent Technologies, Palo Alto, CA). Thus, acquired array images were analyzed using Genepix Pro 4.1 (Axon Instruments, Inc., Foster City, CA). DNA spots were automatically segmented, the local background was subtracted, and the total intensities and fluorescence intensity ratio of the two dyes for each spot were calculated. Fluorescence intensity ratio of the two dyes (Cy3 intensity/Cy5 intensity) were converted into $\log_2$ intensity ratios ($\log_2$ ratio).

For the array used in this study, six simultaneous hybridizations of normal male *versus* normal male were performed to define the normal variation for $\log_2$ ratio. In this experiment, 122 clones showed less than one-tenth the fluorescence intensity of the mean value for all of the clones, and were excluded from array CGH analysis. The remaining 1,966 clones were used for the array CGH analysis. More than 95% of the measured fluorescence $\log_2$ ratio values of each spot (2 × 1966 clones) ranged from +0.2 to −0.2. The thresholds for the $\log_2$ ratio of gains and losses were set at the $\log_2$ ratio of +0.2 and −0.2, respectively. We also normalized the $\log_2$ ratio of each sample according to the following method.

The medium $\log_2$ ratio value for all of the clones was computed, and the clones were selected with a $\log_2$ ratio more than "the median + SD × A " or less than " the median − SD × A." "A" was visually defined as the normal region by referring to the $\log_2$ ratio plots of all clones for each experiment. "A" was also assigned an approximate ranged from 0.3 to 0.7. We then computed the mean $\log_2$ ratio value for the selected clones, and designated this mean $\log_2$ ratio value as " X." Finally, we obtained the "Y" value by subtracting "X" from the $\log_2$ ratio for each clone. In this study, each $\log_2$ ratio was analyzed on the basis of the "Y" value. We visually selected the clones, computed the SD for each experiment, and confirmed that the SD did not exceed 0.15. If it did, the value was considered unreliable for CGH analyses.

Array-hybridization of normal male *versus* normal female was performed to check any change in one copy number of the X chromosome. To confirm linearity associated with a change in the copy number, we also performed array hybridization of normal *versus* each cell line with different number of the X chromosome (GM04626: 47XXX; GM01415D: 48XXXX; and GM05009C: 49XXXXX). These cell lines were obtained from the National Institute of General Medical Sciences Human Genetics Cell Repository Coriell Institute for Medical Research. Fifty seven BAC or PAC clones of the X chromosome were used for the analysis. We computed the mean $\log_2$ ratio value of those clones on each hybridization.

FISH Analysis. We confirmed the location of BAC clones on 13q31-q32 from information archived by the Ensembl Genome Data Resources.[5] FISH analysis using 19 BAC clones located around the region of high-level amplification of 13q31-q32 demonstrated by array CGH, covering ~15 Mb, was used for three cell lines (Karpas 1718, OCI-Ly4, and Rec1). Each interphase chromosome slide of cell lines was prepared according to a standard method. FISH was carried out according to the method described elsewhere (25).

Location of ESTs and Genes. ESTs and genes located on the region of chromosome 13q31.3 were referenced by the National Center for Biotechnology Information,[6] the Ensembl genome data resource,[5] and the University of California at Santa Cruz Biotechnology.[7] Array CGH and FISH analysis demonstrated that the common region of amplification at 13q31-q32 extended from BAC, RP11–360A9 to BAC, RP11–93M14. This region contained 65 independent ESTs that do not overlap each other and *GPC5* (Table 1).

Reverse Transcription-PCR (RT-PCR) Analysis. Three cell lines, Rec1, Karpas 1718, and OCI-Ly4, which showed high amplification on 13q31.3 by FISH and array CGH, were used for RT-PCR analysis. cDNA derived from fetal brain was also included. To avoid amplification from contaminated genomic DNA in the RNA samples, RNA was treated with amplification grade DNaseI (Invitrogen Life Technologies, Inc.) before cDNA syntheses of the samples, which were performed using SuperScriptII (Life Technologies, Inc., Division of Life Technologies, Inc., Gaithersburg, MD). Briefly, each 5 μl of total RNA was reverse-transcribed into cDNA dissolved in 40 μl of distilled water. RT-PCR was performed for 65 ESTs and *GPC5* using the specific primers (Table 1). Each primer was also designed so that the Tm value would be between 55°C and 60°C. Amplifications were performed on a Thermal Cycler (Perkin-Elmer Corporation, Norwalk, CT). RT-PCR was conducted with the touchdown PCR method described elsewhere (26). Briefly, the reactions were comprised of 10 cycles of denaturation (94°C, 0.5 min), annealing (63°C, 0.5 min, 1°C decrease per 2 cycles), and extension (72°C, 2.5 min), followed by 35 cycles of denaturation (94°C, 0.5 min), annealing (58°C, 0.5 min), and extension (72°C, 2.5 min), and a final extension of 5 min at 72°C. Basically, the annealing temperature of the reaction was from 63 to 58°C. Additionally, RT-PCR was also performed under different conditions by changing the annealing temperature from 65 to 60°C or 60°C to 55°C. If no PCR products were obtained, we designed new primer sets to confirm their true negativity. All of the PCR products were separated by electrophoresis and purified using the QIA Quick Gel Extraction kit (Qiagen). TA cloning to purified PCR products was performed by using pBluescriptII SK (−), and sequenced by using ABI PRISM 310 Genetic Analyzer (Applied Biosystems, Foster City, CA).

Northern Blot Analysis. Northern blotting was performed with 30 ESTs and *GPC5* cDNA against five cell lines (Rec1, Karpas 1718, OCI-Ly4, Jurkat, and ATN-1) and human placenta. Additional analysis used the candidate genes BC040320 and *GPC5*, which was included because it has been reported to be a candidate gene for this region (15). We analyzed and compared the expression of each of the ESTs and *GPC5* in the cell lines with high-level amplification at 13q31-q32 (Rec1, Karpas 1718, and OCI-Ly4) and in the cell lines without (Jurkat and ATN-1). To examine the expression of BC040320 and *GPC5* in detail, Northern blot analysis was also performed for several cell lines and patients. Northern blot hybridization was performed with a standard method (21). Each RT-PCR product was used as a specific probe labeled by PCR. Briefly, 10 ng of the RT-PCR products were labeled with [α-^{32}P]dCTP by PCR. The reactions were carried out with 25 cycles of denaturation (94°C, 0.5 min), annealing (55°C, 0.5 min), and extension (72°C, 2.5 min), and a final extension of 5 min at 72°C. Total cellular RNA (5 μg) was size-fractioned on 1% agarose/0.66 M formaldehyde gel, transferred onto a Hybond-N$^+$ nylon membrane (Amersham Pharmacia Biotech, Tokyo, Japan). The membranes were then hybridized overnight at 42°C with [α-^{32}P]dCTP-labeled probes, washed, and then exposed to BIOMAX MS films (EKC, Rochester, NY).

[5] Internet address: http://www.ensembl.org/.
[6] Internet address: http://www.ncbi.nlm.nih.gov/.
[7] Internet address: http://genome.ucsc.edu/.

Downloaded from cancerres.aacrjournals.org on March 4, 2021. © 2004 American Association for Cancer

Table 1 *RT-PCR*[a] *analysis*

BAC clones, EST and STS Marker refer to the information obtained from Ensembl genome data resource. All BAC clones are included in RPCI-11 human male BAC library.

BAC	EST/gene	STS Marker	Forward primer	Reverse primer	FB	Rec1	Karpas 1718	OCI-Ly4
360A9	AW664738	D13S1457	5′-gccacatggtcaggttaaac	5′-cttcactaccttgcgactct	−	ND	ND	−
27D9	AA309162		5′-ggctctcatttagctaaatg	5′-aagaagtggttgagacaaca	+[b]	+	+	+
15N8	No EST							
321E13	AW236754	D13S1175	5′-gagatggcacagcagttgaa	5′-tagttcaaactctacctgca	−	ND	ND	−
447M23	No EST							
370B1	LOC121723		5′-aactactggtgaggactgca	5′-caagttccccttctgcagaa	−	ND	ND	−
	AW059867		5′-aaggcttagctattatgctg	5′-acaatgaggaaaatctccca	++[c]	++	++	++
275J18	BC042969	D13S1818	5′-ctggtcacacatccacaatg	5′-cagtggaatctgagtcctag	++	+	+	++
	AA628299		5′-cagaaggagtgttaagtctg	5′-caagaagaagctgccagtat	++	++	++	++
143O10	No EST							
309H8	BG183515	D13S1239	5′-ctcatgactgtaatcccagc	5′-gtgatgccgtgaaatgagtc	+	+	+	+
	BG191981		5′-ttcagtgacctcactgactg	5′-gaggattttgcagtcatcgc	−	ND	ND	−
114G1	LOC160824	D13S767	5′-aggttttgtcagccacacct	5′-gaactatccgtaccttgtcc	−	++	+	+
75N6	AA398228		5′-ctgtaccattgtgcccagaa	5′-atgactcagtccttctggct	−	ND	ND	−
86C3	No EST	D13S265						
51A2	No EST							
18M3	No EST							
388D4	LOC144774		5′-cactgtggcagttatacggt	5′-caatggttttccgcaccagt	−	ND	ND	−
	LOC121727		5′-cctgggaaggatggtttctt	5′-ttacaacacaaggggcacac	+	+	+	++
409J23	No EST							
392A19	LOC121729		5′-ggagccattacttcaagacc	5′-agaccagtacttgtccagct	+	++	++	++
	BG776186		5′-tggacacgtgagtgtgtttc	5′-atgagctcaggcagctctat	+	++	−	+
	LOC121728		5′-tgataggagacagacctgac	5′-tccagtcatcctgaggtaga	−	ND	ND	−
	BG186078		5′-tcacacagtgtgactcacag	5′-tgatctcctctctgtagtgc	ND	−	−	+
	AA487882		5′-acccaagggaatattgacac	5′-gaagctagggaagcagtatt	ND	−	−	+
	BM542991		5′-tgcagtaggtggcaatctca	5′-tcgacttggactccatgaga	−	ND	ND	−
505P2	BM695971	D13S1234	5′-ccttggagtgcttaaggtag	5′-actagggctctttgtagacc	ND	−	−	++
158A8	AI027278		5′-gctgtgattgcgaagaagtg	5′-tccatatgtgagtgtggcag	ND	−	−	+
	BG927281		5′-acgccaagctctaatacgac	5′-ctcgggctatggtatatgac	−	ND	ND	−
	BI825411		5′-accctggacaggtatggaat	5′-accatgagcacagtgctcaa	−	ND	ND	−
	AA888411		5′-ctcccattgcagttactatg	5′-gtcgacatgttgttgaggtt	+	+	+	+
360H15	AW515966		5′-atgttcaccaggctggtctt	5′-actaactctgtgggcttgca	−	ND	ND	−
	BF818219		5′-tctgcccactaacatctggt	5′-cttgagtagctgagaccaca	−	ND	ND	−
114C3	No EST							
432D3	LOC144776	D13S1190	5′-cacttccttgaaggggtttc	5′-ctctgactcttgggcacaat	ND	+	+	+
	AI126313		5′-ttgagacacagtcctgctct	5′-gcagggcacaatgttttcag	−	ND	ND	−
319L6	AV731092		5′-attggtgaagccacctcaaa	5′-caggctaacatggatctagt	ND	−	−	+
	BG941714		5′-agtgcctacttcctaagacc	5′-tcaggaatcagtgcccaaac	ND	−	−	+
	AI262947		5′-ttgtgttcctggtccaccta	5′-acattgggccggtcacttat	ND	−	−	+
	AI493127		5′-tcaaatcaactgcacctcag	5′-cagttcgagacttcttccat	−	ND	ND	−
51B13	BX097335		5′-gaagtaggatggtgacacct	5′-ctcagcaagtcatcctttgc	−	ND	ND	−
430K10	AL701000	D13S886	5′-tggcctggagtaattagctg	5′-atttaggggtaggagagca	ND	−	−	+
	LOC160827		5′-ctgtgcactatcacttggga	5′-taggctctaagccgttggtt	−	ND	ND	−
	LOC160826		5′-atggaatcaggttccctcca	5′-ctgttcccttcatctgaatg	−	ND	ND	−
	BQ477330		5′-caaagtgctgggattacagg	5′-gccagctttgctgcacatta	−	ND	ND	−
	BQ477741		5′-caacagaagatcggcccttt	5′-actccctgaagcacagcatt	ND	+	+	+
	AV731847		5′-caggcacttgcttaagggat	5′-aactagcctgcttcagcttc	−	ND	ND	−
	BI481522		5′-atgtgaagagaggtctcagc	5′-agcaaaccacctagaggctt	ND	+	+	+
	BU729287		5′-cttagcctaatctccctaggcgga	5′-tatcaggtaggtggtccagtctca	ND	++	++	++
	BM703078		5′-caggatcttgccctgttagt	5′-tatcgggtggcgaacaagat	ND	+	+	+
	AA719672		5′-tgtccttaggtagacattgt	5′-ttcaacctctgagaaaccca	ND	ND	ND	−
	LOC121734		5′-acttcactgtcaacagcgag	5′-agagaccacatgcttgccat	ND	++	++	++
	BE466687		5′-agttctggaggctaaaagtccagt	5′-gccaaaatcacatggagagactac	ND	+	+	+
282D2	BF352993		5′-gagaacagtaatttctttcc	5′-tgcaattattggggtaaagc	ND	ND	ND	−
	BC040320		5′-gtcatacacgtggacctaac	5′-ctgaagtctcaagtgggcat	ND	++	++	++
121J7	AF339828		5′-ctgacaagttctcagatcac	5′-actctgcatgagcctagatt	ND	++	++	++
	AA701926		5′-agaccctgatggtctcttta	5′-ggctcaatgttttcctacgg	ND	++	++	++
	BF908089		5′-tggaagaaaggacatgaggt	5′-tctcatgaatccatgcccaa	ND	+	+	+
	AW868481		5′-aagtaaatgtgagaagtagc	5′-tgctcatcctcattgtata	ND	−	−	+
	BX107378		5′-taacctgagcagaatccagccttg	5′-atggacccaaatgctgagaggaac	ND	++	++	++
	AA599001		5′-aagaggacttgctgtgttg	5′-tgcacagacggtacagaagt	ND	++	++	+
	GPC5		5′-cactggcgggtaaaggggac	5′-agtattcagggaactgtcagtcacacc	ND	+	+	+
	AL043638		5′-ccagtctatcattgatggac	5′-gaagtgcctctgtaattgga	ND	++	++	++
	AL708734		5′-gtaatcccagcactttggga	5′-tcttgttcttgtcccccagt	ND	+	+	+
487A2	AF339802	D13S1490	5′-tacctgggtaaccaagactc	5′-ctctgttcactgcattgaag	ND	++	++	++
	H56919		5′-tgttgaccgactgagtgaac	5′-ttatggtgaagtccttcccc	ND	+	+	++
	AA705439		5′-cgtactctagagttaaccaa	5′-atgattgtaagttccctgag	ND	++	++	++
	W86832		5′-atcctcatttctcaggggct	5′-cctgtctgctctatgaagct	ND	−	−	−
	N49442		5′-tggctgggcagaaatctgaa	5′-tacaggtctgttcgccacat	ND	++	++	++
	N33596		5′-tccctagcaatgtgatgtac	5′-ctaaggtattcctaggctca	ND	−	−	+
	T84913		5′-gtagtaggtagaactgtcct	5′-atctacccteggcaattttc	ND	++	++	++
	BU656134		5′-tgctagggctggagtacaat	5′-cattttctcttggctcaccc	ND	++	++	++
93M14	AW105449		5′-ccagcaactgtaatacatgc	5′-tcttcaaatccttgcctctg	ND	−	+	++
	AV754681		5′-acagccttctttggagagtg	5′-tccaagggcacagtggaatt	ND	−	++	++

[a] RT-PCR, reverse transcription-PCR; BAC, bacterial artificial chromosome; EST, expressed sequence tag; FB, fetal brain; ND, not done; STS, sequenced tagged site.
[b] Detection of a thin band from the result of electrophoresis.
[c] Detection of a thick band from the result of electrophoresis.

Downloaded from cancerres.aacrjournals.org on March 4, 2021. © 2004 American Association for Cancer

Candidate Gene Analysis. BC040320, a candidate gene in the 13q31-q32 amplification region, was additionally analyzed. To confirm the sequence of the candidate gene, RT-PCR was performed between exon 1 and exon 4 of BC040320 using the primers 5′-TCCGGTCGTAGTAAAGCGCAGGCG-3′, designed on the side of exon1 and 5′-CTGAAGTCTCAAGTGGGCAT-3′, designed on the side of exon4 of BC040320. The PCR reaction was the same as the one described in the RT-PCR section.

RESULTS

Array CGH Analysis. Array CGH consisting of 1,966 BAC and PAC clones were examined with normal male *versus* female, and demonstrated that most of the signals from autosomal chromosomes are within $\log_2$ ratio of +0.2 to −0.2 (Fig. 1*A*). The linearity of copy number changes was studied with cell lines having a different number of X chromosomes. As shown in Fig. 1*B*, the result of the plot of each calculated mean fluorescence ratio demonstrated that the fluorescence ratio was proportional to the change of one copy number. The array CGH used for four cell lines (Karpas 1718, Rec1, OCI-Ly4, and OCI-Ly7) and one DLBCL patient (D778) demonstrated high-level gains in copy number changes at 13q31-q32. Fig. 2*A* shows a representative result for Karpas 1718 of the array CGH. Detailed results of chromosome 13 from three cell lines (Karpas 1718, Rec1, and OCI-Ly7) and one DLBCL patient (D778) are shown in Fig. 2*B*. Conventional CGH and FISH analyses clearly confirmed these array CGH data (Fig. 3).

The Common Region of Amplification at 13q31-q32. In an attempt to narrow the amplicon at 13q31-q32, FISH analysis of three cell lines (Karpas 1718, Rec1, and OCI-Ly4), using 19 BAC/PAC probes located on 13q31-q32 (Fig. 4*A*) were conducted, and it was found that the common amplified region at 13q31-q32 was located between RP11–29C8 and RP11–93M14. The high-resolution array CGH data are shown in Fig. 4*B*. Karpas 1718 and D778 (DLBCL patient sample) showed a wide area of amplification extending over >50 Mb of chromosome 13q. A small genomic region showing high-level amplification (defined as $\log_2$ ratio >1) extended from 13q22.2 to 13q31.3, with the region of 13q31.3 in particular showing a higher $\log_2$ ratio of >2. In the same manner, OCI-Ly7 and Rec1 also showed high-level amplification, which confined to 13q31.3. These results identified the common region of high-level amplification to extend from RP11–360A9 to RP11–481A22. On the basis of the FISH and array CGH results, we defined the genomic region between RP11–360A9 and RP11–93M14 as the common and smallest region of amplification in four cell lines and one DLBCL patient.

RT-PCR Analysis for ESTs of Chromosome 13q31.3. Expression of 65 ESTs and *GPC5* located in the common region of amplification on 13q31.3 were examined by RT-PCR using cDNA derived from three cell lines (Karpas 1718, OCI-Ly4, and Rec1) and fetal brain. RT-PCR products were examined by gel electrophoresis. A positive signal was defined as detection of an expected size of band. The results are summarized in Table 1. Thirty ESTs and *GPC5*, which showed the expected size of band, were found to be positive in all of the three cell lines with amplification of 13q31.3, and they were confirmed by their nucleotide sequence. Fifteen ESTs also showed the

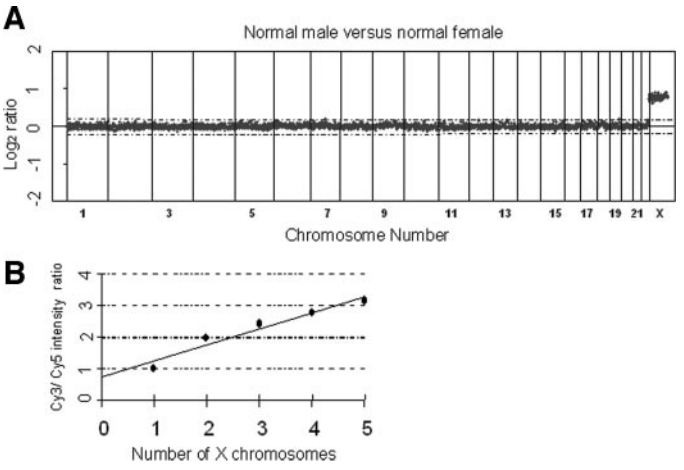

Fig. 1. Array comparative genomic hybridization analysis of normal *versus* female. *A*, representative genomic profile of an array comparative genomic hybridization using normal male *versus* normal female DNAs. Six simultaneous hybridizations of normal male *versus* normal male were performed to define the normal variation in $\log_2$ ratio ($\log_2$ cy3/cy5). In the control experiment, >95% of the measured fluorescence $\log_2$ ratio values of each spot (2 × 1966 clones) ranged from +0.2 to −0.2 (data not shown). The thresholds for the $\log_2$ ratio of gains and loss were therefore set at $\log_2$ ratio of +0.2 and −0.2, respectively. Array data are plotted as the mean $\log_2$ ratio of duplicate spots for each clone. Vertical lines show the threshold for the $\log_2$ ratio of gains and loss. The $\log_2$ ratio for each of the bacterial artificial chromosome clone is plotted as a function of its genome location, with chromosome 1 to the left and X to the right; for each chromosome the order is short-arm telomeric to long-arm telomeric. *B*, normalized $\log_2$ ratio for the changes in copy number of X chromosome. The normal male DNA was used as reference for all hybridizations. Array hybridizations were performed with the test genomic DNA from a normal male (1 × chromosome), a normal female (2 × chromosomes), and three cell lines containing three, four, and five copies of the X chromosome. Each plot stands for the mean value of all normalized fluorescence ratio of 57 clones from the X chromosome. The ratio on each of the X chromosome clone was normalized by the mean fluorescence intensity ratio of autosomal chromosome clones. We defined the fluorescence intensity ratio of array-hybridization with normal male *versus* normal male as 0. Each plot was then computed on the basis of the normalized value. The line represents the linear regression through all of the data with a slope of 0.51 and an intercept of 0.72.

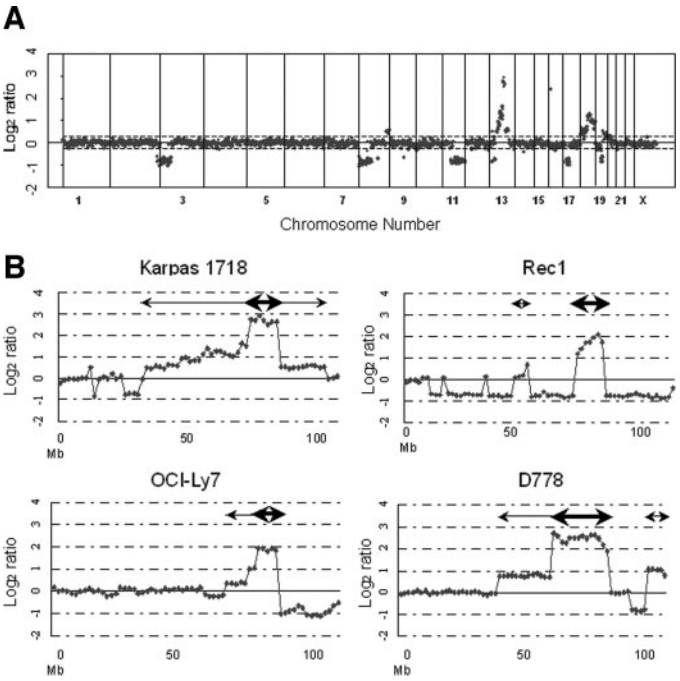

Fig. 2. Genomic profiles of array comparative genomic hybridization. *A*, the representative genomic profile of array comparative genomic hybridization with Karpas 1718. The bacterial artificial chromosomes are ordered by position in the genome beginning at the 1p telomere and ending at the Xq telomere. The *black arrow* above the graph indicates high-level amplification (defined as $\log_2$ ratio >1). *B*, detailed genomic profiles of chromosome 13 in the three cell lines (Karpas 1718, Rec1, and OCI-Ly7) and one diffuse large B cell lymphoma patient (D778). The $\log_2$ ratio for each of the 68 bacterial artificial chromosomes and P-1 derived artificial chromosome clones is plotted as a function of its genome location, with chromosome 13q-centromere to the *left* and 13q-telomere to the *right*. ····, show the threshold for gains and loss. *Bold arrows* indicate high-level amplification (defined as $\log_2$ ratio >1) and *thin arrows* moderate-level amplification ($0.2 > \log_2$ ratio >1). Karpas 1718 shows a wide region of amplification extending over >50-Mb of chromosome 13q. Furthermore, high-level amplification in Karpas 1718 is observed from 13q22.2 to 13q31.3, with 13q31.3 in particular showing the highest amplification ($\log_2$ ratio >2). In the same manner, high-level amplification of OCI-Ly7 and Rec1 are shown at 13q31.3. Rec1 also shows wide loss in the vicinity of 13q31.3. The patient sample (D778) shows a wide region of amplification at 13q21.2–13q31.3 and 13q33.3-qter, with 13q31.1-q31.3 in particular indicating high-level amplification.

Downloaded from cancerres.aacrjournals.org on March 4, 2021. © 2004 American Association for Cancer

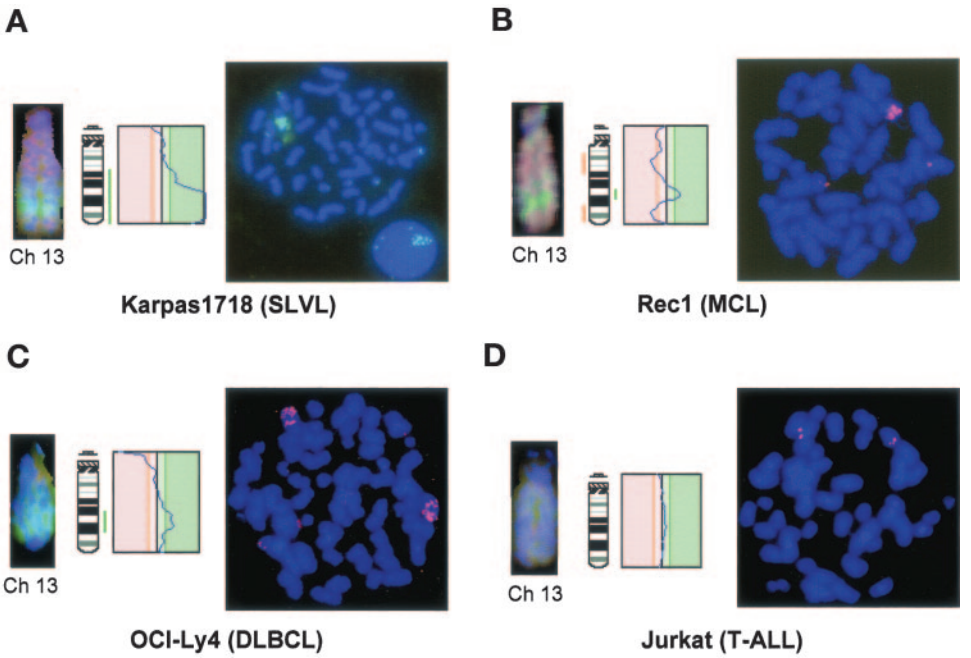

Fig. 3. Fluorescent *in situ* hybridization (FISH) and comparative genomic hybridization (CGH) analysis of cell lines with or without amplification at 13q31-q32. CGH results for four cell lines (Karpas 1718, Rec1, OCI-Ly4, and Jurkat) are shown. The lines to the right (*green*) and to the left (*red*) of each chromosome indicate the region gained or lost, respectively. Representative results of metaphase FISH with bacterial artificial chromosome, RP11–487A2 are shown on the *right side of each panel*. Chromosome 13 examined by CGH is also shown beside each ideogram. Three B-cell lymphoma cell lines, Karpas 1718 (*A*), Rec1 (*B*), and OCI-Ly4 (*C*) show amplification at 13q31-q32, but Jurkat (*D*) does not show one. FISH analysis shows amplification in >15 copies in the three B-cell lines, but no amplification in Jurkat. Each metaphase chromosome was counterstained by 4′,6-diamidino-2-phenylindole.

expected size, but RT-PCR analysis demonstrated only one or two cell lines so that they were excluded as candidate ESTs associated with amplification at 13q31.3. The remaining 21 ESTs did not show any bands in either OCI-Ly4 or fetal brain. They were also examined with another set of primers, but again no bands were detected (data not shown) so that they were also excluded as the candidate ESTs. A total of 35 of 65 ESTs were thus excluded and not additionally analyzed.

Northern Blotting. To identify the expression patterns of 30 ESTs and *GPC5*, Northern blot was used for six kinds of RNAs, which were human placenta, three B-cell lymphoma cell lines (Rec1, Karpas 1718, and OCI-Ly4) with 13q31.3 amplification, and two T-cell lymphoma cell lines (Jurkat and ATN-1) without 13q31.3 amplification. Twenty-two of the ESTs showed hardly any detectable bands in any of the cell lines (Table 2). Fig. 5 shows representative expression patterns of the ESTs. AF339828 and BC040320 showed the similar expression pattern of a transcript of ~6 kb and a smeary band >6 kb. The signals were observed in only three B-cell lymphoma cell lines, but not in human placenta or the T-cell lines. *GPC5*, a gene incompletely included in the common region of amplification at 13q31-q32, showed weak expression of ~5-kb transcript in all of the cell lines and the human placenta at similar intensity. The signals for the other ESTs did not reflect any difference in copy number at 13q31.3 between cell lines and human placenta. Therefore, we regarded AF339828 and BC040320 as the most possible target gene for amplification at 13q31.3. Additional study against various samples including patient samples and normal tissues was performed with these two ESTs, and *GPC5*, reportedly a target gene for 13q31.3 amplification, was also examined.

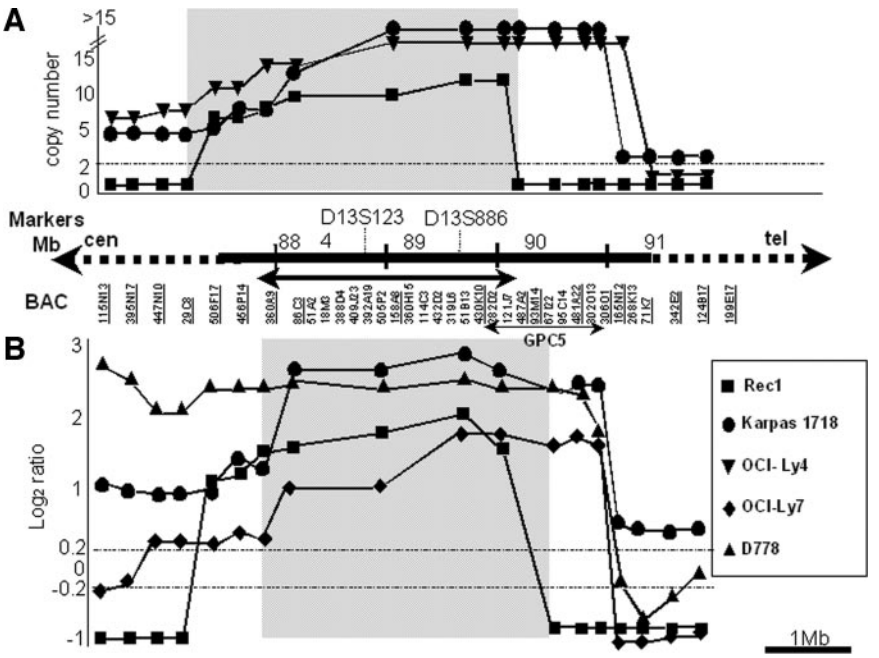

Fig. 4. Analysis of 13q31-q32 by a combination of array comparative genomic hybridization (CGH) and interphase fluorescent *in situ* hybridization (FISH). *A*, summarized data of DNA sequence copy numbers in three cell lines (*Karpas 1718, OCI-Ly4,* and *Rec1*) determined by interphase FISH using 19 bacterial artificial chromosome (BAC) clones of 13q31.3, including a new BAC, RP11–93M14, that was not used for array CGH. Ten interphase cells were analyzed and the average copy numbers of the BAC clone signals were counted for each cell line. The *vertical line* indicates the copy number and the *horizontal dotted line* indicates normal two copies. ▨ shows the common region of gain in copy number, which extended fromRP11–29C8 to RP11–93M14. The positions of STS markers and all BAC clones were confirmed from information archived by Ensembl Genome Data Resource.[5] The underlined BAC clones were used for FISH and array CGH. The *thin arrow* indicates the *GPC5* gene loci. *B*, summarized data of array CGH analysis of three cell lines (*Rec1, Karpas 1718,* and *OCI-Ly7*) and one DLBCL patient (*D778*). The *vertical line* shows $\log_2$ ratio. ···· show the threshold for gain and loss set at $\log_2$ ratios of +0.2 and −0.2, respectively. ▨ shows the common region of high-level amplification ($\log_2$ ratio >1) in the three cell lines, which is extended from RP11–360A9 to RP11–481A22.

Downloaded from cancerres.aacrjournals.org on March 4, 2021. © 2004 American Association for Cancer

Table 2 *Northern blot analysis*

Each signal of those ESTs[a] and GPC-5 was visually evaluated after 1-week expose.

BAC	EST/gene	Probe size (bp)	Size (kb)	Northern Blot					
				Placenta	Rec1	Karpas 1718	OCI-Ly4	Jurkat	ATN-1
RP11-27D9	AA309162	130	−	−	−	−	−	−	−
RP11-370B1	AW059867	160	−	−	−	−	−	−	−
RP11-275J18	BC042969	440	−	−	−	−	−	−	−
	AA628299	220	−	−	−	−	−	−	−
RP11-309H8	BG183515	440	−	−	−	−	−	−	−
RP11-114G1	LOC160824	550	6.5	+++	+++++	++++	+++	+++	+++
RP11-388D4	LOC121727	420	−	−	−	−	−	−	−
RP11-392A19	LOC121729	350	1.5	+	−	−	−	−	−
RP11-158A8	AA888411	300	−	−	−	−	−	−	−
RP11-432D3	LOC144776	500	−	−	−	−	−	−	−
RP11-430K10	BQ477741	240	−	−	−	−	−	−	−
	BI481522	210	5.5	+	++	++	+	++	+
	BU729287	460		+	−	−	−	−	−
	BM703078	470	−	−	−	−	−	−	−
	LOC121734	240	0.8	+	+++	++	++	++	+++
	BE466687	390	−	−	−	−	−	−	−
RP11-282D2	BC040320	400	6	−	+++++	+++++	+++++	−	−
RP11-121J7	AF339828	410	6	−	+++++	+++++	+++++	+/−	−
	AA701926	240	−	−	−	−	−	−	−
	BF908089	100	−	−	−	−	−	−	−
	BX107378	420	−	−	−	−	−	−	−
	AA599001	200	−	−	−	−	−	−	−
	GPC5	600	5	+	+	+	+	+	+
	AL043638	200		−	−	−	−	−	−
	AL708734	250	−	−	−	−	−	−	−
RP11-487A2	AF339802	320	6	+/−	++	++	++	+	+
	H56919	160	−	−	−	−	−	−	−
	AA705439	290	15	+	++	+	+++	+/−	+/−
	N49442	320	15	+	++	+	+++	+/−	+/−
	T84913	200	−	−	−	−	−	−	−
	BU656134	390	−	−	−	−	−	−	−

[a] EST, expression sequence tag; BAC, bacterial artificial chromosome.

Northern blot results with the BC040320 probe are shown in Fig. 6. High-level expression of BC040320 was seen in five cell lines with amplification at 13q31-q32 (Rec1, Karpas 1718, OCI-Ly4, OCI-Ly7, and OCI-Ly8). Lower level of expression than that of the five cell lines was seen in three cell lines without amplification (Karpas 422, SP49, and SUDHL6). Furthermore, two patients with amplification showed higher expression than the other two patients without amplification. These results indicated that the expression of BC040320 paralleled the gain in copy number shown by both conventional and array CGH. On the same membrane, expression of *GPC5* in five cell lines with amplification at 13q31-q32 was not significantly different from that of the other cell lines without amplification, suggesting that *GPC5* is not a likely candidate gene. The expression pattern of BC040320 was examined against various hematopoietic cell lines (T-cell lymphoma, multiple myeloma, myeloid leukemia, and natural killer/T-cell lymphoma; Fig. 6*B*). Some cell lines showed weak signals when compared with the two cell lines with high-level amplification. *GPC5* cDNA again yielded very weak signals without significant differences but with some variation. When normal tissues were examined, the BC040320 signal was hardly observable except for lung, thymus, and lymph node (Fig. 6*C*).

In conclusion, the result of Northern blot using each of the probes revealed that the expression of BC040320 paralleled the gain in copy

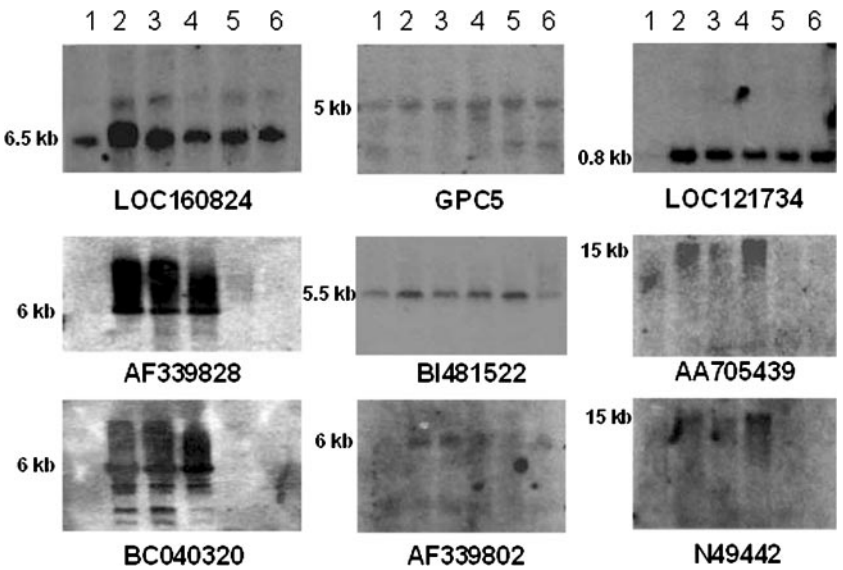

Fig. 5. Northern blot analysis of the candidate gene for 13q31-q32 amplification. Northern hybridization was performed against 6 kinds of RNAs comprising human placenta (*lane 1*), 3 B-cell lymphoma cell lines (*lane 2*, Rec1; *lane 3*, Karpas 1718; and *lane 4*, OCI-Ly4) with amplification at 13q31-q32 and 2 T-cell lymphoma cell lines (*lane 5,* Jurkat and *lane 6,* ATN-1) without amplification. Representative and characteristic expression patterns of 8 of 30 ESTs and *GPC5* are shown. Expression of *GPC5* and BI481522 was not significantly different, whereas LOC160824, AF339828, BC040320, AF339802, LOC121734, AA705439, and N49442 showed clearly different patterns of expression. In particular, the expression of AF339828 and BC040320, which showed similar patterns of hybridization, demonstrates concordance with the gain in copy number at 13q31-q32.

Downloaded from cancerres.aacrjournals.org on March 4, 2021. © 2004 American Association for Cancer

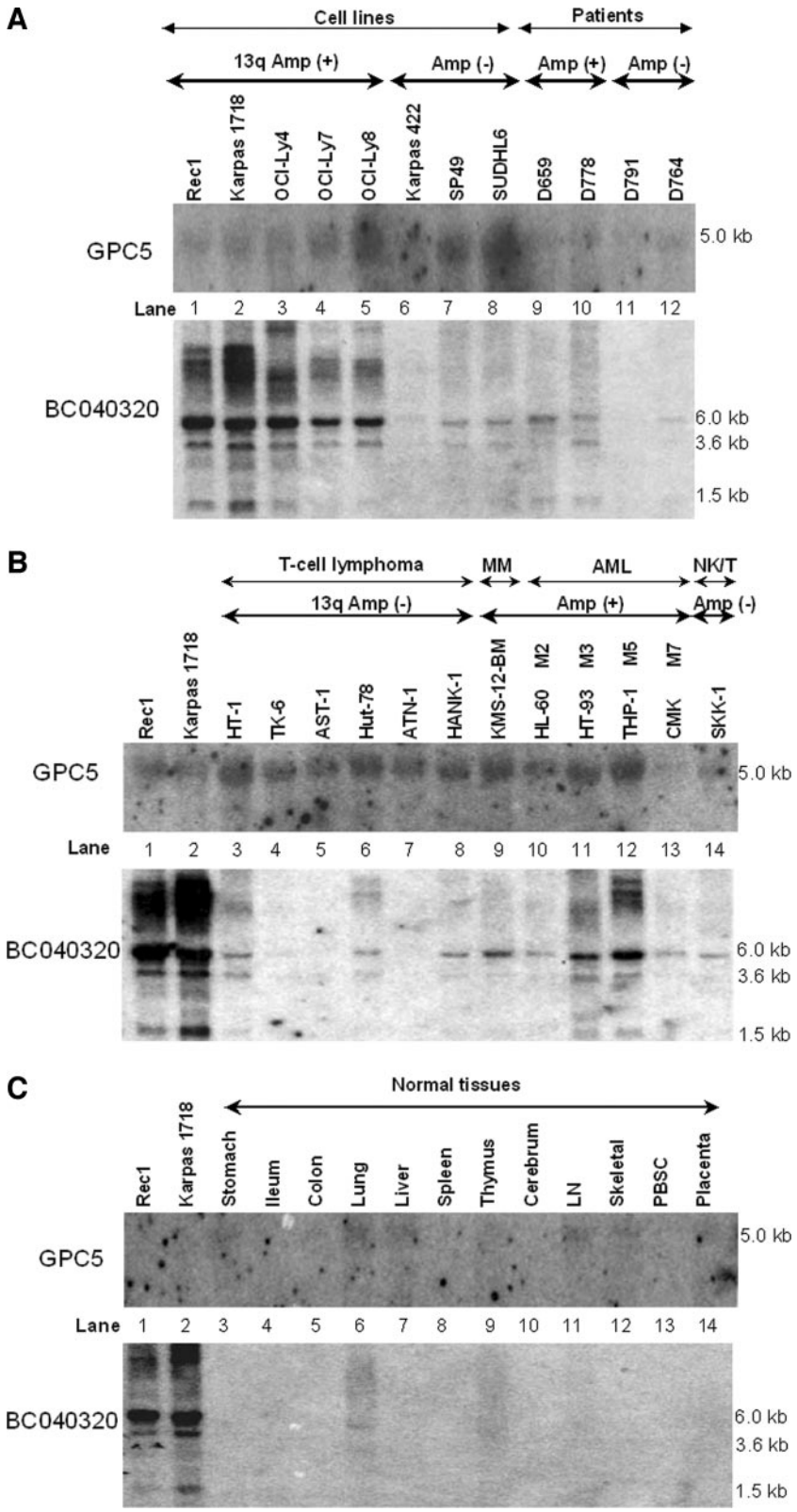

Fig. 6. Expression study of *GPC5* and BC040320. Amplification status at 13q31-q32 in each of the cell lines and diffuse large B-cell lymphoma (DLBCL) patients examined by conventional comparative genomic hybridization is indicated above names of the samples. *A*, expression pattern of *GPC5* and BC040320 in cell lines and DLBCL patients with or without amplification at 13q31-q32. Expression of *GPC5* in five cell lines and two DLBCL patients with amplification at 13q31-q32 is not significantly different from that of the other cell lines and patients without amplification. BC040320 is expressed in cell lines with amplification at 13q31-q32 (*lanes 1–5*) and at much lower levels in cell lines without amplification (*lanes 6–8*). In the same manner, BC040320 is strongly expressed in DLBCL patients with amplification at 13q31-q32 (*lanes 9* and *10*), but very weakly in cell lines without amplification (*lanes 11* and *12*). *B*, expression pattern of *GPC5* and BC040320 in multiple cell lines with hematopoietic malignancies. Some cell lines (*lanes 9, 11,* and *12*) with amplification at 13q31-q32 show weak signals when compared with the two cell lines (*lanes 1* and *2*) with high-level amplification. Expression of *GPC5* shows very weak signals with some variations but without significant differences. *AML,* acute myeloid leukemia cell line. *MM,* multiple myeloma cell line. *NK/T,* natural killer/T-cell lymphoma/leukemia cell line. *C*, expression pattern of BC040320 and *GPC5* in multiple normal tissues. Expression of BC040320 is hardly visible in normal tissues except for lung, thymus, and lymph node when compared with that of the two cell lines (*lanes 1* and *2*) with high-level amplification at 13q31-q32.

number at 13q31-q32 and that BC040320 was, thus, most likely to be the candidate gene.

Full Length, Genomic Location, and Characterization of the Candidate Gene. We focused on AF339828 and BC040320 as the most likely candidate gene on the basis of the results of FISH, array CGH, and Northern blot analysis. We named this candidate gene *C13orf25* (*Chromosome 13 open reading frame 25*) according to the recommendation of HUGO Gene Nomenclature Committee.[8]

[8] Internet address: http://www.gene.ucl.ac.uk/nomenclature/.

Downloaded from cancerres.aacrjournals.org on March 4, 2021. © 2004 American Association for Cancer

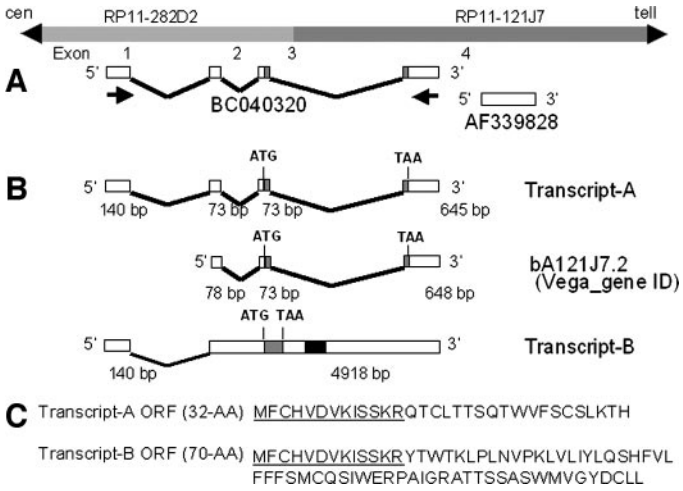

Fig. 7. Exon-intron structure of the *C13orf25* gene. *A*, two expressed sequence tags, BC040320 and AF339828, which are overexpressed in the cell lines with amplification at 13q31.3, are shown above the ····. BC040320 is split into four exons, encompassing two bacterial artificial chromosome clones, RP11–282D2 and RP11–121J7. AF339828 is located to the telomeric side of BC040320 and ~300-bp apart from BC040320. The primer set used for reverse transcription-PCR is shown below the exons. *B*, two transcripts obtained by reverse transcription-PCR. One (*Transcript-A*) is the same as the BC040320 sequence consisting of four exons containing 965-bp nucleotides. The other (*Transcript-B*) consists of two exons containing 5058-bp nucleotides. Computer analysis showed that 32-AA polypeptides of bA121J7.2 (*Vega gene ID*) were encoded in the Transcript-A cDNA. Possible open reading frames are shown as ▨. Five precursor microRNAs (miRNAs; miR91-precursor-13 micro RNA, miR18- precursor-13 micro RNA, miR19a- precursor-13 micro RNA, miR19b- precursor-13 micro RNA, and miR92-precursor-13 micro RNA), including seven mature microRNAs (microRNA miR-17, miR-91, miR-18, miR-19a, miR-20, miR-19b, and miR-92) were obtained from the Transcript-B sequence, and are shown by the ■ in Transcript-B. *C*, polypeptides sequences are also shown below the structure. The polypeptides of 13 amino acids (*AA*) are shared by Transcript-A and Transcript-B, and are indicated by *underlining*.

To additionally characterize this gene and cDNA structures, we performed RT-PCR on exon 1 to exon 4 of BC040320. Two transcripts were obtained and sequence analysis found the shorter one to be transcript-A and the longer one transcript-B (Fig. 7). Database search with the Vega Genome Browser showed that bA121J7.2 (Vega_gene ID) is also located in this region.[9] The peptides of 32-amino acids (AA) were predicted as bA121J7.2. The peptides of 32-AA predicted in bA121J7.2 were also predicted transcript-A. Furthermore, the same initiation codon predicted the 70-AA polypeptide in the transcript-B. It should be noted that five kinds of precursor microRNAs (miRNAs; miR91-precursor-13 micro RNA, miR18- precursor-13 micro RNA, miR19a-precursor-13 micro RNA, miR19b-precursor-13 micro RNA, and miR92-precursor-13 micro RNA), including seven kinds of miRNA (microRNA miR-17, miR-91, miR-18, miR-19a, miR-20, miR-19b, and miR-92) were also recognized in the sequence of transcript-B (Fig. 7).

DISCUSSION

Genetic alteration in 13q has been reported in many human cancers, including hematopoietic malignancies. Recent molecular genetic studies using FISH and CGH have demonstrated that amplification at 13q31-q32 has been detected frequently in hematopoietic malignancies. Amplification at 13q21-qter was demonstrated frequently in B-cell malignancies (5–8). *GPC5* has been proposed recently as the candidate gene for 13q31-q32 amplification region in B-cell lymphoma cell lines (15). In the study reported here, we examined genomic alteration at the *GPC5* loci using array CGH and the expression of *GPC5* using Northern blotting. The *GPC5* sequence in the 2-Mb genomic region at 13q31.3 approximately ranges from BAC, RP11–121J7 to BAC, RP11–268K13. Our array CGH data for Rec1 showed that the $\log_2$ ratio of BAC, RP11–481A22, which located the intron of *GPC5* between exon 6 and exon 7, showed a loss in copy number ($\log_2$ ratio = −0.76). The array data indicated that other BACs located on the telomeric side of this BAC also showed a loss. Our FISH data with Rec1 using the new BAC clone, RP11–93M14, containing exon 3, exon 4, and exon 5 of *GPC5*, also showed a loss in copy number. These results demonstrated that the *GPC5* locus was not fully included in the common region of amplification at 13q31-q32 in the cell lines, suggesting that *GPC5* in this allele might not be functional.

Northern blotting also showed that expression of *GPC5* in cell lines with amplification at 13q31-q32 was not significantly different from that of the other cell lines without amplification. On the other hand, both BC040320 and AF339828 were expressed only in B-cell lymphoma cell lines with 13q31-q32 amplification but not in T-cell lymphoma or human placenta without 13q31-q32 amplification. Their ESTs were fully included in the common region of amplification at 13q31-q32. Detailed analysis using Northern blot showed that the expression of BC040320 almost paralleled the gains in copy number shown by both conventional and array CGH. Northern blot analysis showed that BC040320 was especially overexpressed in B-cell lymphoma cell lines with amplification at 13q31-q32 and hardly expressed in normal tissues, including lymphoid tissues. Although we also found minor mRNA expression of BC040320 in SP49 (mantle cell lymphoma cell line) and SUDHL6 (B-cell lymphoma cell line) without amplification at 13q31-q32 (Fig. 6*B*), this expression may well have been caused not by the gain in copy number but other reasons that are not yet fully understood. These results suggested that BC040320 was the most likely a candidate gene for the amplification at 13q31-q32. We named this candidate gene *C13orf25* (*Chromosome 13 open reading frame 25*).

To confirm the validity of *C13orf25* cDNA, RT-PCR was performed, and two transcripts (Transcript-A and -B) were obtained. The Vega genome browser[9] predicted the presence of a gene, *bA121J7.2*, encoding 32-AA polypeptides in the Transcript-A cDNA. A possible open reading frame in Transcript-B was also predicted, encoding 70-AA polypeptides starting from the same ATG (Fig. 7). The genomic structure of *C13orf25* might be incomplete on the 3′ side because AF339828, which showed the same pattern of hybridization as BC040320, was observed near *C13orf25* and was located at 300-bp downstream of *C13orf25*. Because of the presence of multiple bands in Northern blot analysis with BC040320, various transcripts might also be produced, but RT-PCR demonstrated major transcripts. The result of computer analysis using National Center for Biotechnology Information BLAST[10] showed that the predicted proteins of *C13orf25* contained no putative domains in those transcripts. Further study is needed, however, to characterize the proteins.

Five precursor miRNAs (miR91-precursor-13 miRNA, miR18-precursor-13 miRNA, miR19a-precursor-13 miRNA, miR19b-precursor-13 miRNA, and miR92-precursor-13 miRNA), including seven mature miRNAs (miRNA miR-17, miR-91, miR-18, miR-19a, miR-20, miR-19b, and miR-92), were obtained from the transcript-B sequence. The function of miRNA reportedly is to regulate the expression of target genes in both humans (27) and *Caenorhabditis elegans* (28–31). miRNAs also mediate a cleavage of mRNA in *Arabidopsis thaliana* (32, 33). Calin *et al.* (34) reported recently an association between chronic lymphocytic leukemia and deletion of a section of chromosome 13 that contains the genes for miR-15 and miR-16. The

[9] Internet address: http://vega.sanger.ac.uk/.

[10] Internet address: http://www.ncbi.nlm.nih.gov/BLAST/.

Downloaded from cancerres.aacrjournals.org on March 4, 2021. © 2004 American Association for Cancer

presence of these miRNAs on the *C13orf25* gene may provide an insight into the processes of tumorigenesis.

In the study presented here, we were able to demonstrate that *C13orf25* but not *GPC5* is the most likely candidate gene for amplification. *C13orf25* gene was expressed in association with genomic amplification, and may play an important role in tumorigenesis and resulting poor prognosis.

Additional investigation into the function of *C13orf25*, including the seven miRNAs, can be expected to provide an insight into the role of the *C13orf25* in tumorigenesis.

ACKNOWLEDGMENTS

We thank Drs. Wen-Lin Kuo and Joe Gray at University of California at San Francisco (San Francisco, CA) for kindly sending us a detailed protocol of array CGH. The outstanding technical assistance of Hiroko Suzuki and Yumiko Kasugai is also very much appreciated. Encouragement and advice of Mitsuo Kawase at Nihon Insulator, Inc. for array CGH technology are also acknowledged.

REFERENCES

1. Schwab M. Oncogene amplification in solid tumors. Semin Cancer Biol 1999;9:319–25.
2. Schwab M. Amplification of N-Myc as a prognostic marker for patients with neuroblastoma. Semin Cancer Biol 1993;4:13–8.
3. Brodeur GM, Seeger RC, Schwab M, Varmus HE, Bishop JM. Amplification of N-MYC in untreated human neuroblastomas correlates with advanced diseased stage. Science (Wash. DC) 1984;224:1121–4.
4. Slamon DJ, Clark G, Wong SG, Levin WJ, Ullrich A, McGuire WL. Human breast cancer: correlation of relapse and survival with amplification of the HER-2/neu oncogene. Science 1987;235:177–82.
5. Rao PH, Houldsworth J, Dyomina K, et al. Chromosomal and gene amplification in diffuse large B-cell lymphoma. Blood 1998;92:234–40.
6. Monni O, Oinonen R, Elonen E, et al. Gain of 3q and deletion of 11q22 are frequant abverrations in mantle cell lymphoma Genes Chromosomes Cancer 1998;21:298–307.
7. Neat MJ, Foot N, Jenner M, et al. Localization of novel region of recurrent amplification in follicular lymphoma to an ~6.8 Mb region of 13q32–33. Genes Chromosomes Cancer 2001;32:236–43.
8. Mao X, Lillington D, Child F, Russell-Jones R, Young B, Whittaker S. Comparative genomic hybridization analysis of primary cutaneous B-cell lymphoma: identification of common genomic alterations in disease pathogenesis. Genes Chromosomes Cancer 2002;35:144–55.
9. Ko YH, Choi KE, Han JH, Kim JM, Ree HJ. Comparative genomic hybridization stud of nasal-type NK/T-cell lymphoma. Cytometry 2001;46:85–91.
10. Knuutila S, Bjorkqvist A-M, Autio K, et al. DNA copy number amplifications in human neoplasms. Am J Pathol 1998;152:1107–23.
11. Schmidt H, Wurl P, Taubert H, et al. Genomic imbalances of 7p and17q in malignant peripheral nerve sheath tumors are clinically relevant. Genes Chromosomes Cancer 1999;25:205–11.
12. Lallamendy ML, Tarkkanen M, Blomqvist C, et al. Compatative genomic hybridization of malignant fibrous histiocytoma reveals a novel prognostic marker. Am J Pathol 1997;151:1153–61.
13. Gordon AT, Brinkschmidt C, Anderson J, et al. A novel and consistent amplicon at 13q31 associated with alveolar rhabdomyosarcoma. Genes Chromosomes Cancer 2000;28:220–6.
14. Karnan S, Tagawa H, Suzuki R, et al. Analysis of chromosomal imbalances in de novo CD5-positive diffuse large-B-cell lymphoma detected by comparative genomic hybridization. Genes Chromosomes Cancer 2004;39:77–81.
15. Yu W, Inoue J, Imoto I, Matsuo Y, Karpas A, Inazawa J. GPC5 is a possible target for the 13q31–q32 amplification detected in lymphoma cell lines. J Hum Genet 2003;48:331–5.
16. Solinas-Toldo S, Lampel S, Stilgenbauer S, et al. Matrix-based comparative genomic hybridization: biochip to screen for genomic imbalance. Genes Chromosomes Cancer 1997;20:399–407.
17. Pinkel D, Segraves R, Sudar D, et al. High resolution analysis of DNA copy number variation using comparative genomic hybridization to microarray. Nat Genet 1998;23:41–6.
18. Martinez-Climent JA, Alizadeh AA, Segraves R, et al. Transformation of follicular lymphoma to diffuse large cell lymphoma is associated with a heterogeneous set DNA copy number and gene expression alterations. Blood 2003;101:3109–17.
19. Martinez-Climent JA, Vizcarra E, Sanchez D, et al. Loss of a novel tumor suppressor gene locus at chromosome 8p is associated with leukemic mantle cell lymphoma Blood 2001;98:3479–82.
20. Dyer MJ, Fischer P, Nacheva E, Labastide W, Karpas A. A new human B-cell non-Hodgkin's lymphoma cell line (Karpas 422) exhibiting both t(14;18) and t(4;11) chromosomal translocations. Blood 1990;75:709–14.
21. Naoe T, Akao Y, Yamada K, et al. Cytogenetic characterization of a T-cell line, ATN-1, derived from adult T-cell leukemia cells. Cancer Genet Cytogenet 1988;34:77–88.
22. Takizawa J, Suzuki R, Kuroda H, et al. Expression of the TCL1 gene at 14q32 in B-cell malignancies but not in adult T-cell leukemia. Jpn J cancer Res 1998;89:712–8.
23. Hodgson G, Hagar JH, Volik S, et al. Genome scanning with array CGH delineates regional alterations in mouse islet carcinomas. Nat Genet 2001;29:459–64.
24. Hakan T, Nigel-PC, Charloytte E, Magnus N, Bruce AJP, Alan T. Degenerated oligonucleotide-primed PCR: General amplification of target DNA by a single degenerated primer. Genomics 1992;13:718–25.
25. Tagawa H, Karnan S, Kasugai Y, et al. *MASL1*, a candidate oncogene found in amplification at 8p23.1, is translocated in immunoblastic B cell lymphoma cell line OCI-LY8. Oncogene 2004;23:2576–81.
26. Motegi M, Yonezumi M, Suzuki H, et al. API2-MALT1 chimeric transcripts involved in mucosa-associated lymphoid tissue type lymphoma predicted heterogenous products. Am J Pathol 2000;156:807–12.
27. Kawasaki H, Taira K. Hes1 is a target of microRNAs-23 during retinoic-acid-induced neuronal differentiation of NT2 cells. Nature (Lond.) 2003;423:838–42.
28. Lee RC, Feinbaum RL, Ambros V. The C. elegans heterochronic gene lin-4 encodes small RNAs with antisense complementarity to lin-14. Cell 1993;75:843–54.
29. Reinhart BJ, Slack FJ, Basson M, et al. The 21-nucleotide let-7 RNA regulates developmental timing in Caenorhabdtis elegans. Nature (Lond.) 2000;403:901–6.
30. Pasquinelli AE, Reinhart BJ, Slack F, et al. Conservation of the sequence and temporal expression of let-7 hetero chronic regulatory RNA. Nature (Lond.) 2000;408:86–9.
31. Slack FJ, Basson M, Liu Z, Ambros V, Horvitz HR, Ruvkun G. The lin-41 RBCC gene acts in the C. elegans heterochronic pathway between thelet-7 regulatory RNA and the LIN-29 transcriptional factor. Mol Cell 2000;5:659–69.
32. Llave C, Xie Z, Kasschau KD, Carrington JC. Cleavage of Scarecrow-like mRNA targets directed by a class of Arabidopsis miRNA. Science (Wash DC) 2002;297:2053–6.
33. Tang G, Reinhart BJ, Bartel DP, Zamore PD. A biochemical framework for RNA silencing in plants. Genes Dev 2003;17:49–63.
34. Calin GA, Dumitru CD, Shimizu M, et al. Frequent deletions and down-regulation of micro RNA genes miR15 and miR16 at 13q14 in chronic lymphocytic leukemia. Proc Natl Acad Sci USA 2002;99:15534–29.

Downloaded from cancerres.aacrjournals.org on March 4, 2021. © 2004 American Association for Cancer

AACR American Association for Cancer Research

Cancer Research

The Journal of Cancer Research (1916–1930) | The American Journal of Cancer (1931–1940)

Identification and Characterization of a Novel Gene, *C13orf25*, as a Target for 13q31-q32 Amplification in Malignant Lymphoma

Akinobu Ota, Hiroyuki Tagawa, Sivasundaram Karnan, et al.

Cancer Res 2004;64:3087-3095.

Updated version	Access the most recent version of this article at: http://cancerres.aacrjournals.org/content/64/9/3087

Cited articles	This article cites 33 articles, 8 of which you can access for free at: http://cancerres.aacrjournals.org/content/64/9/3087.full#ref-list-1
Citing articles	This article has been cited by 75 HighWire-hosted articles. Access the articles at: http://cancerres.aacrjournals.org/content/64/9/3087.full#related-urls

E-mail alerts	Sign up to receive free email-alerts related to this article or journal.
Reprints and Subscriptions	To order reprints of this article or to subscribe to the journal, contact the AACR Publications Department at pubs@aacr.org.
Permissions	To request permission to re-use all or part of this article, use this link http://cancerres.aacrjournals.org/content/64/9/3087. Click on "Request Permissions" which will take you to the Copyright Clearance Center's (CCC) Rightslink site.

Downloaded from cancerres.aacrjournals.org on March 4, 2021. © 2004 American Association for Cancer Research.